

Alma Mater Studiorum Università di Bologna
Archivio istituzionale della ricerca

Development and software in the loop validation of a Model-based water injection combustion controller for a GDI TC engine

This is the final peer-reviewed author's accepted manuscript (postprint) of the following publication:

Published Version:

Ranuzzi F., Cavina N., Brusa A., De Cesare M., Panciroli M. (2019). Development and software in the loop validation of a Model-based water injection combustion controller for a GDI TC engine. SAE International [10.4271/2019-01-1174].

Availability:

This version is available at: <https://hdl.handle.net/11585/703895> since: 2024-05-10

Published:

DOI: <http://doi.org/10.4271/2019-01-1174>

Terms of use:

Some rights reserved. The terms and conditions for the reuse of this version of the manuscript are specified in the publishing policy. For all terms of use and more information see the publisher's website.

This item was downloaded from IRIS Università di Bologna (<https://cris.unibo.it/>).
When citing, please refer to the published version.

(Article begins on next page)

Development and Software in the Loop Validation of a Model-based Water Injection Combustion Controller for a GDI TC Engine

Author, co-author (Do NOT enter this information. It will be pulled from participant tab in MyTechZone)

Affiliation (Do NOT enter this information. It will be pulled from participant tab in MyTechZone)

Abstract

Turbocharged (TC) engines work at high Indicated Mean Effective Pressure (IMEP), resulting in high in-cylinder pressures and temperatures, improving thermal efficiency, but at the same time increasing the possibility of abnormal combustion events like knock and pre-ignition. To mitigate knocking conditions, engine control systems typically apply spark retard and/or mixture enrichment, which decrease indicated work and increase specific fuel consumption.

Many recent studies have advocated Water Injection (WI) as an approach to replace or supplement existing knock mitigation techniques. Water reduces temperatures in the end gas zone due to its high latent heat of vaporization. Furthermore, water vapor acts as diluent in the combustion process.

In this paper, the development of a novel closed-loop, model-based WI controller is discussed and critically analyzed. The innovative contribution of this paper is to propose a control strategy based on an analytical combustion model that describes the relationship between the combustion phase and the Spark Advance (SA), considering also the effects of the injected water mass. Such model is calibrated with experimental data acquired during dedicated experimental tests on a GDI TC engine, equipped with a prototype Port Water Injection (PWI) system.

At first the WI setup is described, and the main experimental data are presented and processed for model identification. Two algorithm versions are then explained in detail and implemented in Simulink environment, with a Real-Time (RT) oriented approach. In the last part of this work, the WI control strategy is tested in a Software in the Loop (SiL) system, coupled with a one-dimensional Fast Running Engine Model (FRM). The controller is tested on several engine points in steady state and transient conditions and the Root Mean Squared Error (RMSE) is calculated for the control targets. In this way, the performance of the model-based controller is verified, and the two versions of the algorithm are quantitatively compared.

Introduction

Recently, the use of water in internal combustion engines to supplement the air-fuel mixture has rapidly gained relevance for modern boosted and downsized GDI SI engines [1,2,3,4]. At high load these engines are exposed to knock and even preignition or super-knock events, due to high in-cylinder pressure, and therefore engine combustion control is usually designed to retard the combustion phasing. This procedure, in addition to the need to enrich AFR value of the mixture at high power to reduce exhaust gas

temperature, inevitably affects performance and efficiency. Thus, Water Injection is recognized to be one of the key technologies for enabling higher efficiency spark ignited gasoline engines [5,6,7]. Water Injection enables higher compression ratios up to 14 by mitigating heat release rates and knock tendency at high loads. Therefore, optimum spark advance can be maintained over a wider area of engine operating map, relaxing the knock limited spark advance (KLSA) constraint. Furthermore, WI allows reducing thermal stresses on the turbine and exhaust system components, without fuel enrichment. The addition of water produces air cooling due to evaporation and charge dilution (EGR-like), which slows down the combustion rate and reduces peak temperatures [1,2,8,9,10].

In [4] a Port Water Injection experimental setup is described, and an experimental campaign focused on WI effects on combustion is shown. The tests consist in SA sweeps performed for different values of the injected water mass, for each single operating point. The water mass injected in the runners is defined by the parameter r :

$$r = \frac{m_w}{m_f} \quad (1)$$

Where m_w and m_f are the masses of water and fuel introduced during a cycle, respectively. The data analysis shows two fundamental effects related to the increase of r : a gradual reduction of knock intensity close to Maximum Brake Torque (MBT) SA and a proportional delay of combustion phasing. Instead, the MBT value is slightly affected by r variations and there is a little offset of optimum 50% Mass Fraction Burned (MFB50) angle. These results suggest that it is possible to use WI to reduce knock intensity, allowing to achieve the combustion phase that ensures MBT even at high load, without exposing engine to damage. The achievement of this goal requires the identification of the proper combination of r and SA values to be applied at every operating condition. The value of r must be chosen as the smallest value able to guarantee the necessary mitigation of dangerous events to keep knock level under a defined threshold, while MFB50 is maintained at optimum angle. On the other hand, SA must be defined to achieve the optimum MFB50 angle, considering the delay induced by water addition. This paper describes the development of an analytical control-oriented combustion model to ensure the highest combustion efficiency at high load using WI, by the determination of optimal SA values for given operating conditions (engine speed, load and injected water mass). This approach allows implementing such relationship in a simple way, with an extremely low computational effort. In fact, the model is based on the parabolic trend of the MFB50 with respect to the SA, and this can be implemented with fast calculations, which are particularly important for real-time control strategies. On the other hand, the necessity of a 4-dimensional lookup table is avoided (the SA should be mapped on a grid of different values of engine speed,

$$SA_{first} = SAbase + \frac{3*r}{0.2} \quad (5)$$

In which:

- $SAbase$ is the calibration value of SA
- The 3 CA offset has been arbitrarily assumed as the average value of combustion delay related to a step of 0.2 r [4]

In conclusion the SA sweeps are carried out with the following specifications:

1. Angular steps of 3CA from SA_{first} to nKLSA
2. Angular steps of 1 CA from nKLSA to KLSA

This methodology has been conceived to obtain a wide vision of WI effects on MFB50 and, at the same time, to investigate with more accuracy all combustion indexes near the KLSA area.

WI Combustion Model

Experimental data has been processed, point by point, to analyze the relationship between SA and MFB50, for each tested r value. For a single spark sweep, the most appropriate fitting function to analytically describe the relationship between SA and MFB50 is the quadratic polynomial, as clearly shown in Figure 1. Such figure displays some spark sweeps for different values of parameter r , highlighting the influence of such parameter on the trend that could be identified in the absence of water injection.

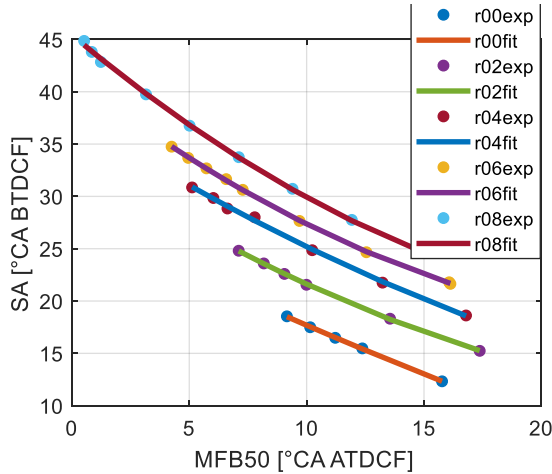


Figure 1. Parabolic fitting of the SA trend with respect to MFB50, for the engine point characterized by $NL=1.2$ and $RPM=2500$, and for different water-to-fuel mass ratios. It is an example of the parabolic trend that links the SA to the MFB50 for fixed operating conditions.

The Equation (6) defines the polynomial fitting of the SA on MFB50 domain.

$$SA = a MFB50^2 + b MFB50 + c \quad (6)$$

This analysis allows to conceive a WI Combustion Model that processes the RPM, NL, r and the target of MFB50 as inputs, to compute the corresponding SA to be applied. The base concept is to calculate the parameters a , b and c of the parabolic function and investigate the analytical dependence of each parameter from the r value. Three different methods have been designed to build such

model, and the respective performances have been evaluated by comparing experimental and modeled SA. The fitting quality has been quantified for each proposed method by evaluating the correlation coefficient.

Polynomial Method

Through the parabolic fitting of MFB50 and SA data for each engine point and for each value of r , the three coefficients a , b , c , (called Parabolic Coefficients), have been identified. Each parameter has been fitted with a polynomial function of RPM and NL (Net Load), for each value of r . The resulting equation for a , b and c is the following:

$$PCoeff = p_{00} + RPM * p_{10} + NL * p_{01} + \dots + RPM * NL * p_{11} + RPM^2 * p_{20} \quad (7)$$

Where p_{00} , p_{10} , p_{01} , p_{11} , p_{20} , are called Surface Coefficients. In Figure 2 are shown all the resulting surfaces, for $r=0$.

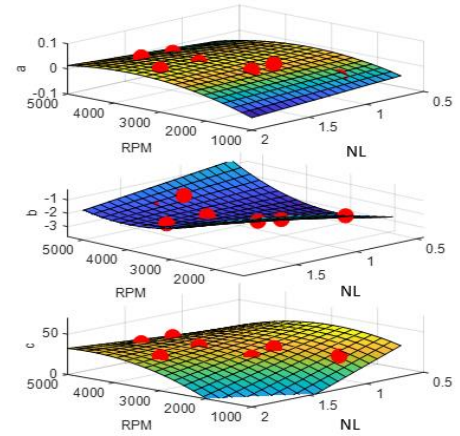


Figure 2. Fitting surfaces of the parabolic coefficients in (RPM, NL) domain, for $r=0$.

Every single surface is described by a set of 5 Surface Coefficients p_{xx} and each coefficient features a quite constant slope in r domain as displayed in Figure 3, so it can be fitted with a linear function, as shown in Eq. (8).

$$p_{xx} = o_{xx} + r * g_{xx} \quad (8)$$

Where o_{xx} is the constant term and g_{xx} the curve slope.

the WI modelling has been modified to be in accordance with the new ducts configuration. As accurately described in a previous work [16], the WI system has been modelled with two injectors, where the first is a Port Water Injector (PWI) and the second is a Direct Water Injector (DWI). Through the calibration of parameters which define how the injected water mass is split between such injectors, the water vapor quantity and the angular duration of in-cylinder water evaporation can be correctly reproduced. Due to the new engine model layout, the WI previous configuration has been replaced with a single DWI layout and the parameters values have been replaced with a new calibration set. Figure 16 shows the layout of the FRM.

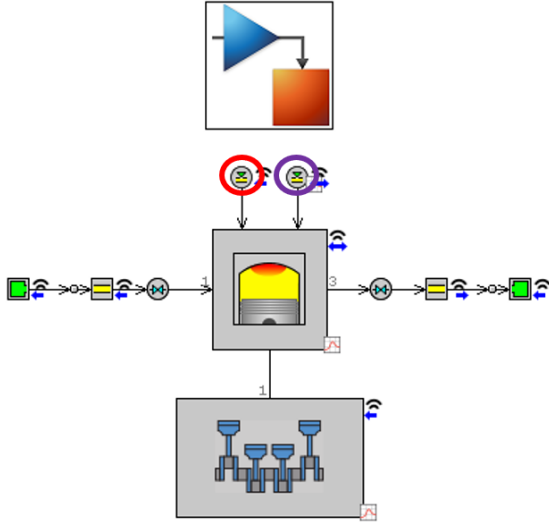


Figure 16. FRM layout. The red circle highlights the Direct Water Injector, the violet one highlights the fuel one.

Simulation Results

The FRM has been appropriately compiled and it has been consequently implemented in a 0-D co-simulation environment. The first simulations allow to identify the best calibration parameters set for the CL controller. They have been carried out for different engine points, in steady state and in transient conditions. During such simulations the PI controller applies r corrections which are then added to the map value, and CL contribution is not saturated above a specific value. This means the final r can assume too high values. Of course, this is not representative of a real application, in which the maximum r is certainly much lower, but such strategy allows studying the PI behavior on r and SA corrections also for high load conditions. It is important to accurately calibrate the CL parameters on the entire operating field.

In Figures 17, 18, 19 and 20 the results of simulations with the first version of the Water Injection based Combustion Control (characterized by the CL on MAPO98) are collected, for four different engine points. In Figure 17, 18 and 19 it has been simulated a medium NL condition and the CL works only with r corrections. In Figure 20 a high load engine point has been simulated and during the firsts 50 cycles it is possible to highlight the protection action with a SA decrement, due to a high MAPO cycle. For small errors on MAPO98 the PI manages the water mass and for high errors introduces also SA variations. The r corrections can have also a negative sign, to reduce the mapped water mass when the recorded MAPO98 is lower than the threshold (Figure 17). The CL parameters set has been chosen to guarantee a good correction stability and, at the same time, fast responses during transients. Figure 21 shows a

transient simulation and during the rising ramp the CL is able to manage the knock intensity only with r corrections. In figures 17 through 21 the error between the mean MFB50 and the map value (the target) is due to inaccuracies of the Water Injection based Combustion Model used in the open-loop controller, which are quantified with the Root Mean Squared Error. The Table 4 collects the RMSE committed by the controller on the MFB50 and MAPO98 targets for each simulation, because they represent the indexes which allow to quantify the controller robustness. The errors are evaluated excluding the firsts cycles, due to the MAPO98 and MFB50 buffers which are filling and do not produce coherent values.

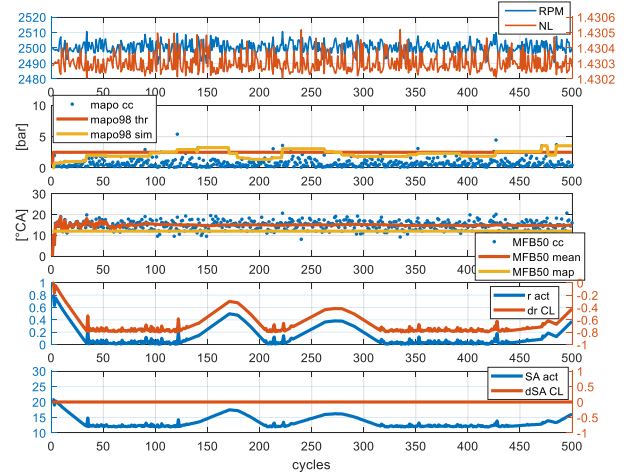


Figure 17. Steady state simulation results for engine point 2500 RPM, NL 1.43. Five subplots show (from top to bottom): RPM-NL, cycle-to-cycle recorded MAPO, MAPO98 and the MAPO98 threshold, cycle-to-cycle recorded MFB50, mean MFB50 and the corresponding target, the actuated r and the r correction calculated by CL chain, the actuated SA and the SA correction calculated by the CL chain.

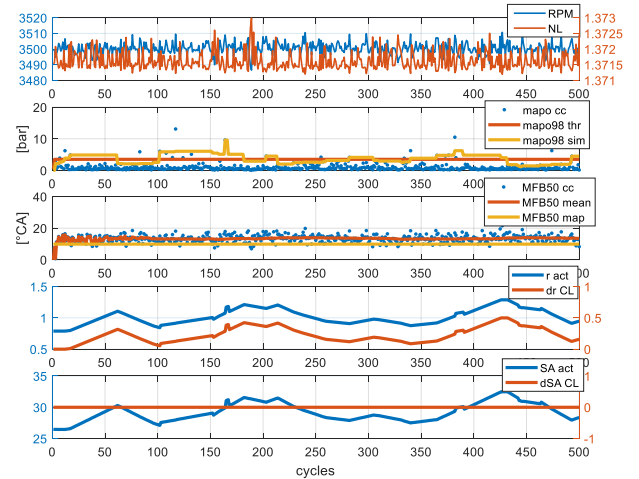


Figure 18. Steady state simulation results for engine point 3500 RPM, NL 1.37. Five subplots show (from top to bottom): RPM-NL cycle-to-cycle recorded MAPO, MAPO98 and the MAPO98 threshold, cycle-to-cycle recorded MFB50, mean MFB50 and the corresponding target, the actuated r and the r correction calculated by CL chain, the actuated SA and the SA correction calculated by the CL chain.

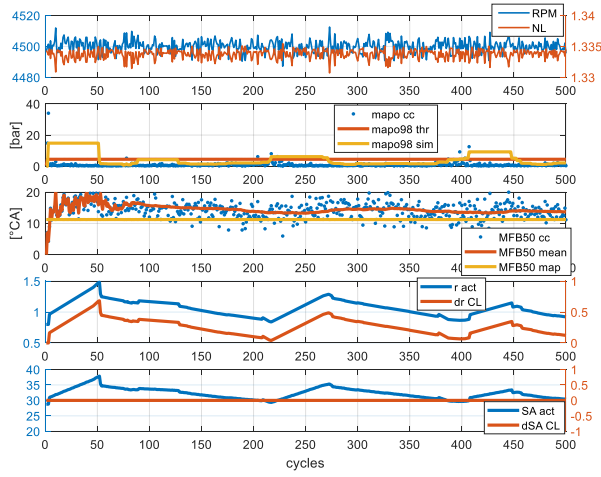


Figure 19. Steady state simulation results for engine point 4500 RPM, NL 1.33. Five subplots show (from top to bottom): RPM-NL, cycle-to-cycle recorded MAPO, MAPO98 and the MAPO98 threshold, cycle-to-cycle recorded MFB50, mean MFB50 and the corresponding target, the actuated r and the r correction calculated by CL chain, the actuated SA and the SA correction calculated by the CL chain.

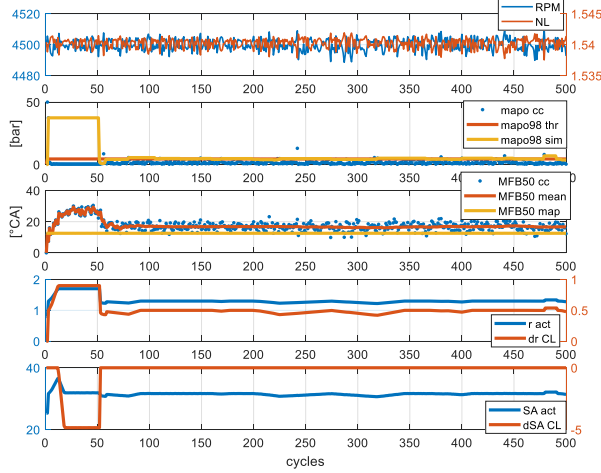


Figure 20. Steady state simulation results for engine point 4500 RPM, NL 1.54. Five subplots show (from top to bottom): RPM-NL cycle-to-cycle recorded MAPO, MAPO98 and the MAPO98 threshold, cycle-to-cycle recorded MFB50, mean MFB50 and the corresponding target, the actuated r and the r correction calculated by CL chain, the actuated SA and the SA correction calculated by the CL chain.

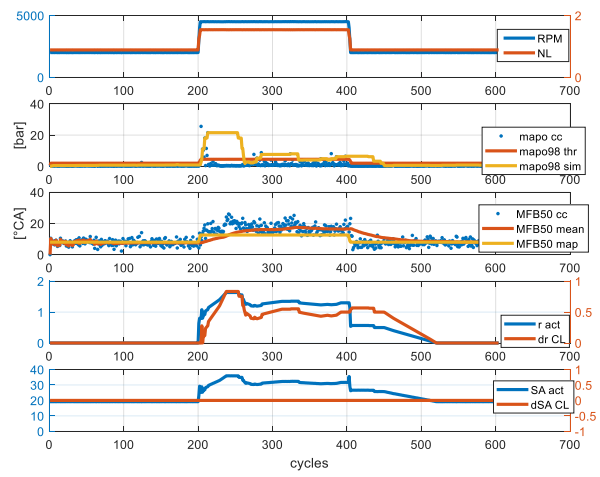


Figure 21. Transient simulation results. Five subplots show (from top to bottom): RPM-NL, cycle-to-cycle recorded MAPO, MAPO98 and the MAPO98 threshold, cycle-to-cycle recorded MFB50, mean MFB50 and the corresponding target, the actuated r and the r correction calculated by CL chain, the actuated SA and the SA correction calculated by the CL chain.

Table 4. Root Mean Squared Errors for the validation simulations with the first version of the WI based Combustion Control. The mean value of the RMSE on mean (by moving average) MFB50 represents the accuracy of the Combustion Model.

Engine Point	RMSE MFB50 [°CA]	RMSE MAPO98 [bar]
RPM 2500 NL 1.43	1.81	0.55
RPM 3500 NL 1.37	2.55	1.24
RPM 4500 NL 1.33	2.10	0.63
RPM 4500 NL 1.54	1.61	0.81
RPM 2000-4500-2000 NL 0.8-1.7-0.8	1.75	4.02
Mean	1.96	1.45

Results of simulations with the second version of WICC (characterized by CL on MAPO98 and MFB50 target) are shown in Figures 22, 23, 24, 25 and 26. The CL on MAPO98 parameters values does not change, but during these simulations the final SA correction is the sum of two contributions (from MAPO98 and MFB50 CL controllers). The positive SA corrections are accepted only when the TPC is under a predetermined value. In Figure 24 it is possible to highlight negative and quick SA corrections in correspondence with a cycle characterized by a high MAPO level. In fact, in such simulation, the high MAPO value produces a high lower saturation of TPC, which is translated in an upper saturation of MFB50TPC to manage measured knock levels. This system avoids also on-off CL responses. In both figures it can be clearly seen that the MFB50 target is reached by the control system, thanks to the closed loop corrections evaluated by the MFB50 CL controller. The Figure 26 shows the transient simulation result during which the controller is able to maintain the mean MFB50 on the corresponding target. The CL calibration parameters have been set on values which guarantees fast responses of the controller to have quite fast

responses also in few simulated cycles, at the expense of the best stability. The Table 5 collects the RMSE for all simulations. The values highlight the reduction of the error on the MFB50 target.

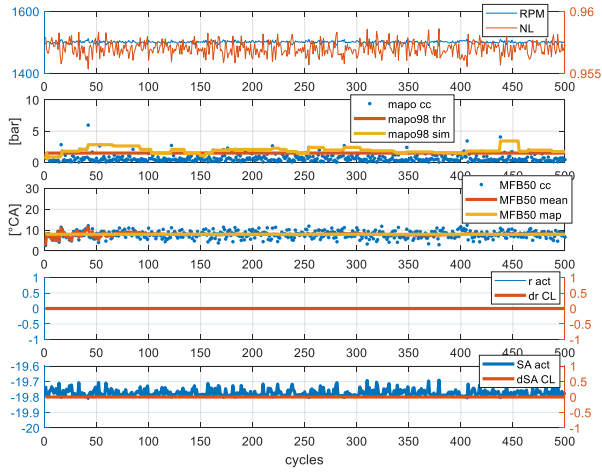


Figure 22. Steady state simulation results for engine point 1500 RPM, NL 0.95 with the CL on MFB50. Five subplots show (from top to bottom): cycle-to-cycle recorded MAPO, MAPO98 and the MAPO98 threshold, cycle-to-cycle recorded MFB50, mean MFB50 and the corresponding target, the actuated r and the r correction calculated by CL chain, the actuated SA and the SA correction calculated by the CL chain.

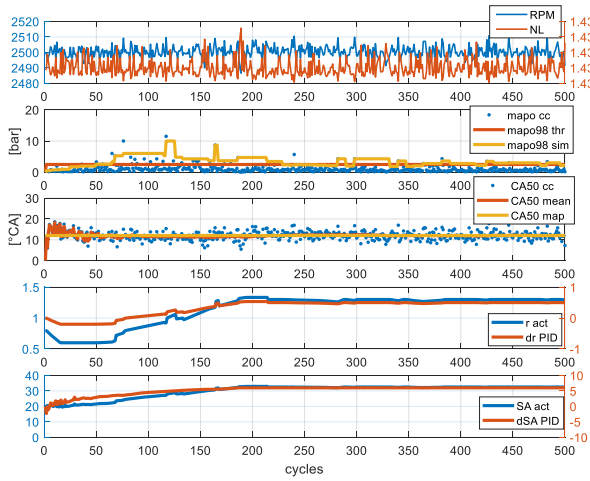


Figure 23. Steady state simulation results for engine point 2500 RPM, NL 1.43 with the CL on MFB50. Five subplots show (from top to bottom): cycle-to-cycle recorded MAPO, MAPO98 and the MAPO98 threshold, cycle-to-cycle recorded MFB50, mean MFB50 and the corresponding target, the actuated r and the r correction calculated by CL chain, the actuated SA and the SA correction calculated by the CL chain.

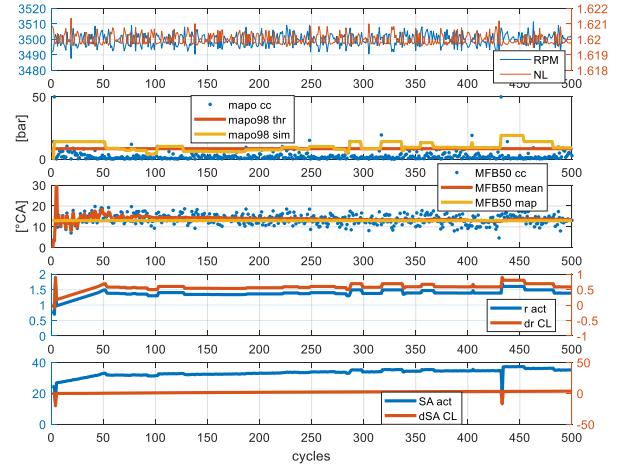


Figure 24. Steady state simulation results for engine point 3500 RPM, NL 1.62 with the CL on MFB50. Five subplots show (from top to bottom): RPM-NL, cycle-to-cycle recorded MAPO, MAPO98 and the MAPO98 threshold, cycle-to-cycle recorded MFB50, mean MFB50 and the corresponding target, the actuated r and the r correction calculated by CL chain, the actuated SA and the SA correction calculated by the CL chain.

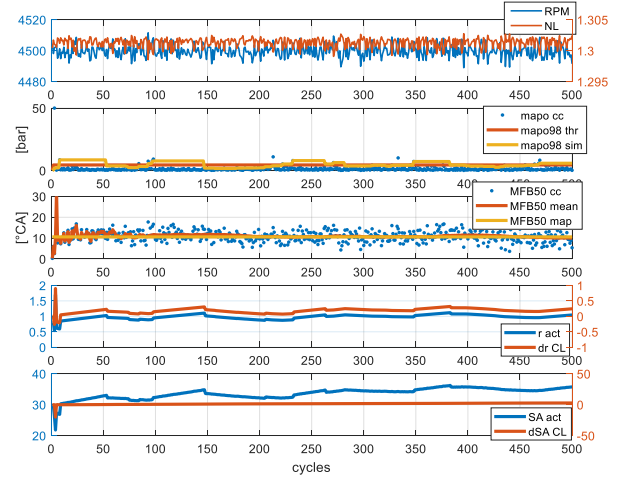


Figure 25. Steady state simulation results for engine point 4500 RPM, NL 1.3 with the CL on MFB50. Five subplots show (from top to bottom): RPM-NL cycle-to-cycle recorded MAPO, MAPO98 and the MAPO98 threshold, cycle-to-cycle recorded MFB50, mean MFB50 and the corresponding target, the actuated r and the r correction calculated by CL chain, the actuated SA and the SA correction calculated by the CL chain.

8. Rahimi Boldaji, M., Sofianopoulos, A., Mamalis, S., and Lawler, B., "Effects of Mass, Pressure, and Timing of Injection on the Efficiency and Emissions Characteristics of TSCI Combustion with Direct Water Injection," SAE Technical Paper 2018-01-0178, 2018, doi:10.4271/2018-01-0178.
9. Netzer, C., Franken, T., Seidel, L., Lehtiniemi, H. et al., "Numerical Analysis of the Impact of Water Injection on Combustion and Thermodynamics in a Gasoline Engine using Detailed Chemistry," SAE Technical Paper 2018-01-0200, 2018, doi:10.4271/2018-01-0200.
10. Pauer, T., Martin Frohnmaier, M., Walther, J., Schenk, P., Hettinger, A., Kampmann, R., "Optimization of Gasoline Engines by Water Injection", Internationales Wiener Motorensymposium 2016.
11. Xiao, B., Wang, S., Prucka, R.G., "A Semi-Physical Artificial Neural Network for Feed Forward Ignition Timing Control of Multi-Fuel SI Engines", SAE Technical Paper 2013-01-0324, 2013, doi:10.4271/2013-01-0324
12. Hillion, M., Chauvin, J., Petit, N., "Open-Loop Combustion Timing Control of a Spark-Ignited Engine," Proceedings of the 47th IEEE Conference on Decision and Control, pp 5635-5642, 2008.
13. Wang, S., Prucka, M., Dourra, H., "Model-Based Optimal Combustion Phasing Control Strategy for Spark Ignition Engines", SAE Technical Paper 2016-01-0818, 2016, doi:10.4271/2016-01-0818
14. Businaro, A., Cavina, N., Corti, E., Mancini, G., Moro, D., Ponti, F., Ravaglioli, V., "Accelerometer Based Methodology for Combustion Parameters Estimation", Energy Procedia, Volume 81, December 2015, Pages 950-959, <https://doi.org/10.1016/j.egypro.2015.12.152>
15. Gamma Technology Inc., GT Gamma Technology, 2017.
16. Cavina, N., Brusa, A., Rojo, N., and Corti, E., "Statistical Analysis of Knock Intensity Probability Distribution and Development of 0-D Predictive Knock Model for a SI TC Engine," SAE Technical Paper 2018-01-0858, 2018, doi:10.4271/2018-01-0858.

MFB50TPC	Total Percentage Correction that derives from MFB50 error
nKLSA	near Knock Limited Spark Advance
NL	Net Load
OL	Open Loop
PI	Proportional Integral Controller
RMSE	Root Mean Squared Error
RT	Real Time
SA	Spark Advance
SiL	Software in the Loop
TPA	Three Pressure Analysis
TPC	Total Percentage Correction
WI	Water Injection
WICC	Water Injection based Combustion Control
WICM	Water Injection based Combustion Model

Abbreviations

CC	Cycle-to-Cycle
CCV	Cycle to-Cycle Variability
CL	Closed Loop
FRM	Fast Running Model.
KLSA	Knock Limited Spark Advance
MAPO	Maximum Amplitude of Pressure Oscillations
MAPO98	98 th MAPO percentile
MAPO98 th	98 th MAPO percentile threshold
MBT	Maximum Brake Torque
MFB50	Angle corresponding to 50% of Mass Fraction Burned